Smart Structures and Systems, *Vol. 15, No. 5 (2015) 1203-1214*
DOI: http://dx.doi.org/10.12989/sss.2015.15.5.1203

Force identification by using specific forms of PVDF patches

Simon Chesné[*1] and Charles Pézerat[2]

[1]*Lyon University, CNRS INSA-Lyon, LaMCoS UMR5259, Rue des Sciences, F-69621, Villeurbanne France*
[2]*LUNAM, Maine University, CNRS UMR 6613, LAUM (Ensim), Avenue Olivier Messiaen, 72085 LE MANS CEDEX 9, France*

(Received October 8, 2013, Revised February 7, 2014, Accepted February 9, 2014)

Abstract. This paper deals with the experimental validation of the use of PVDF Patches for the assessment of spatial derivatives of displacement field. It focuses more exactly on the shear **F**orce **I**dentification by using **S**pecific forms of PVDF patc**H**es (FISH) on beams. An overview of the theoretical approach is exposed. The principle is based on the use of the weak form of the equation of motion of the beam which allows the shear forces to be extracted at one edge of the sensor when this last has a specific form. The experimental validation is carried out with a cantilever steel beam, excited by a shaker at its free boundary. The validation consists in comparing the shear force measured by the designed sensor glued at the free edge and the directly measured force applied by the shaker. The sensor is made of two patches, called the "stiffness" patch and the "mass" patch. The use of both patches allows one to identify correctly the shear force on a large frequency domain. The use of only the stiffness patch is valid in the low frequency domain and has the advantage to have a frequency-independent gain that allows its use in real time.

Keywords: piezoelectricity; sensors; vibration; indirect measurement

1. Introduction

In many structural dynamic applications, the need to assess to spatial derivatives of displacement fields is recurrent. Indeed, they can be used for the identification of sources (Pezerat and Guyader 1995, Pezerat and Guyader 2000), of structural intensity (Noiseux 1970, Pavic 1976, Gavric and Pavic 1993), of material properties (Ablitzer *et al*. 2012, Chochol *et al*. 2013), of boundary conditions (Chesne *et al*. 2006, Chesne *et al*. 2008) or for fault detections (Xu *et al*. 2011), because they are linked to internal efforts like shear forces and/or bending moments which give precious information of the local dynamic behavior of the structure. Of course, derivation of experimentally obtained distributions is an implementation problem, since it amplifies errors inherent in measurements. Because the displacement field can only be measured at discrete points, the usual derivation techniques consist in applying finite differences (see for example: (Pezerat and Guyader 1995, Pezerat and Guyader 2000, Pavic 1976 or Noiseux 1970) or using expansions of the field in a basis of analytical and differential continuous distributions, like eigen shapes (Pezerat and Guyader 1995), Chebyshev polynomials (Chochol *et al*. 2013), plane waves (Zhang and Mann 1999), etc. Since these operations approximate derivatives, they amplify the measurement noises,

∗Corresponding author, Associate Professor, E-mail: simon.chesne@insa-lyon.fr

http://www.techno-press.org/?journal=sss&subpage=8 ISSN: 1738-1584 (Print), 1738-1991 (Online)

the result must then be regularized by using optimum spacing (Leclere and Pezerat 2012) or optimum truncation (Pezerat and Guyader 1995, Chochol *et al.* 2013) which constitute filtering smoothing the calculated derivatives. When only a derivative is required, a specific sensor could be developed, measuring directly the desired derivative. This is the aim of this work, where the possibilities to design sensors based on PVDF patches are studied. A theoretical approach was proposed by authors in (Chesne and Pezerat 2011). It was developed for beams and uses a local weak form of the equation of motion of the beam with a test distribution. These approaches are close to the Virtual Field Method (VFM) which uses the principle of virtual work to identify mechanical constitutive parameters of materials (Grediac1989, Pierron 2012). The main difference is that the test functions have not to be kinematically admissible. In the scope of force identification, as shown in (Chesne *et al.* 2006 and Chesne *et al.* 2008), the judicious choice of analytical test distributions allows shear forces or bending moments to be calculated at the edges of the integration of the displacement field on a small measurement area. This integration has the advantage to be less sensitive to the uncertainties of measurement; it can also be naturally obtained thanks to the properties of PVDF patches. The spatial filtering property of these PVDF sensors is the subject of many works [Hubbard (2010)] and usually known in case of modal filtering (Lee and Moon 1990, Clark 1996, Gu 1994, Gawronski 2000, Friswell 2001, François 2001, Preumont 2003). The goal of this paper is to show experimental validations of the shear **F**orce **I**dentification by using **S**pecific forms of PVDF patc**H**es (called FISH in the following) on beams. It constitutes then an add on of (Chesne and Pezerat 2011).In order to give an independent reading, a brief overview of the theoretical approach is given in a first part.

2. Overview of the FISH

2.1 Principle of the mathematical shear force extraction

The goal of this section is to give the basic equations used for the **F**orce **I**dentification using **S**ensor patc**H**es (FISH) which is based on the weak form of the equation of motion of the structure. For more details, readers can also refer to the previous article (Chesne and Pezerat 2011). The studied mechanical system is a flexural Euler-Bernoulli beam. Considering a forced harmonic vibration, the equation of motion can be written as follows (Guyader 2006)

$$E_b I \frac{\partial^4 w}{\partial x^4}(x) - \mu\omega^2 w(x) = F(x) \tag{1}$$

where *w(x)* is the harmonic transverse displacement, μ, E_b and *I* are respectively the mass per unit length, the complex Young's modulus and flexural inertia of the beam, *F(x)* is the external force distribution applied along the beam.

Considering only a part of the beam with a local coordinate system $x \in [0, a]$, the weak form of the equation of motion in this subdomain corresponds to the spatial integration of the equation of motion (1) multiplied by a test function $\eta(x)$

$$\int_0^a \eta(x)[E_b I \frac{\partial^4 w}{\partial x^4}(x) - \mu\omega^2 w(x)]dx = \int_0^a \eta(x)F(x)dx. \tag{2}$$

If there is no external excitation in the subdomain, Eq. (2) becomes

$$\int_0^a \eta(x)[E_b I \frac{\partial^4 w}{\partial x^4}(x) - \mu\omega^2 w(x)]dx = 0. \tag{3}$$

Now, if we consider that the test function is equal to the second derivative of another function $\psi(x)$, Eq. (3) can be written as

$$\int_0^a \frac{\partial^2 \Psi}{\partial x^2}(x)[E_b I \frac{\partial^4 w}{\partial x^4}(x) - \mu\omega^2 w(x)]dx = 0. \tag{4}$$

This last equation can then be transformed using three integrations by parts, leading to the following expression

$$\begin{aligned} &\Lambda(a)\frac{\partial^2 \Psi}{\partial x^2}(a) - \Lambda(0)\frac{\partial^2 \Psi}{\partial x^2}(0) - M(a)\frac{\partial^3 \Psi}{\partial x^3}(a) + M(0)\frac{\partial^3 \Psi}{\partial x^3}(0) \\ &-\mu\omega^2 w(a)\frac{\partial \Psi}{\partial x}(a) + \mu\omega^2 w(0)\frac{\partial \Psi}{\partial x}(0) - \mu\omega^2 \frac{\partial w}{\partial x}(a)\Psi(a) + \mu\omega^2 \frac{\partial w}{\partial x}(0)\Psi(0) \\ &= \int_0^a \frac{\partial^2 w}{\partial x^2}(x)[E_b I \frac{\partial^4 \Psi}{\partial x^4}(x) - \mu\omega^2 \Psi(x)]dx, \end{aligned} \tag{5}$$

Where $\Lambda(x)$ is the shear force (proportional to third spatial derivative of the displacement) and *M(x)* is the bending moment (proportional to second spatial derivative of the displacement).

If an appropriate function $\psi(x)$, is chosen in order to verify some boundary conditions at *x=0* and *x=a*, the boundary shear forces ($\Lambda(0)$ or $\Lambda(a)$) can be isolated and directly calculated by the spatial integration of the curvature $\frac{\partial^2 w}{\partial x^2}$ with the analytical function $\left[E_b I\left(\frac{\partial^4 \psi}{\partial x^4} - \mu\omega^2\psi(x)\right)\right]$. For example, in order to extract the shear force at *x=0* (first boundary of the subdomain), the polynomial function

$$\Psi(x) = \frac{1}{2}x^2 - 5x^4/a^2 + 10x^5/a^3 - \frac{15}{2}x^6/a^4 + 2x^7/a^5 \tag{6}$$

is a good candidate since its boundary conditions are

$$\begin{aligned} &\Psi(0) = 0 \quad \Psi(a) = 0, \\ &\frac{\partial \Psi}{\partial x}(0) = 0 \quad \frac{\partial \Psi}{\partial x}(a) = 0, \\ &\frac{\partial^2 \Psi}{\partial x^2}(0) = 1 \quad \frac{\partial^2 \Psi}{\partial x^2}(a) = 0, \\ &\frac{\partial^3 \Psi}{\partial x^3}(0) = 0 \quad \frac{\partial^3 \Psi}{\partial x^3}(a) = 0. \end{aligned} \tag{7}$$

Indeed, in this case, Eq. (5) becomes

$$\Lambda(0) = -\int_0^a \frac{\partial^2 w}{\partial x^2}(x)[E_b I \frac{\partial^4 \Psi}{\partial x^4}(x) - \mu\omega^2 \Psi(x)]dx \tag{8}$$

Note that the shear force $\Lambda(a)$, the bending moments *M(0)* and *M(a)* or the slopes $\frac{\partial w}{\partial x}|_{x=0}$ and $\frac{\partial w}{\partial x}|_{x=a}$ can also be obtained by the same expression of Eq.(8)changing only the expression of the function $\psi(x)$, as detailed in Chesne and Pezerat (2011).

2.2 Use of piezoelectric properties

When considering a piezoelectric laminar sensor, with no skew angle, and a charge amplifier, it is possible to obtain an output voltage proportional to the electric charge in the electrode (see (Hubbard 2010). Consequently, with respect to Euler Bernoulli theory, the delivered signal depends on the integral of the curvature of the patch weighted by its width $b_p(x)$

$$v(t) = A\int_0^a \frac{\partial^2 w}{\partial x^2}(x,t) b_p(x) dx \tag{9}$$

where A is a constant depending of the piezoelectric characteristics of the patch material and the thickness of the beam (see (Chesne and Pezerat 2011) for more details).The comparison of Eqs. (8) and (9) shows that if the width of the patch $b_p(x)$is proportional to $\left[E_b I\left(\frac{\partial^4 \psi}{\partial x^4} - \mu\omega^2\psi(x)\right)\right]$ with $\psi(x)$ given in Eq.(6), the designed sensor delivers a signal proportional to the shear force sensor located at one of its edges.

2.3 Definition of the mass and stiffness patches

The use of the weak form of the equation of motion and the properties of a piezoelectric patch allows the shear force (or bending moment or slope) to be extracted at one frequency only because ω intervenes in the expression of the width. In order to extend the usefulness of the measurement technique to a broader frequency domain, a separation in two different patches is proposed. The first patch has a width proportional to $\psi(x)$. It is called the "mass patch", because it is related to the kinetic energy (see Eq. (10)). The second patch has a width proportional to $\frac{\partial^4 \psi}{\partial x^4}$. It is called the "stiffness patch", related to the strain energy and can be bonded to the opposite side of the beam. Fig. 1 illustrates this specific set-up. Because both patches can be fixed at opposite sides at the same coordinate, the shear force can be obtained from the linear combination of both delivered signals

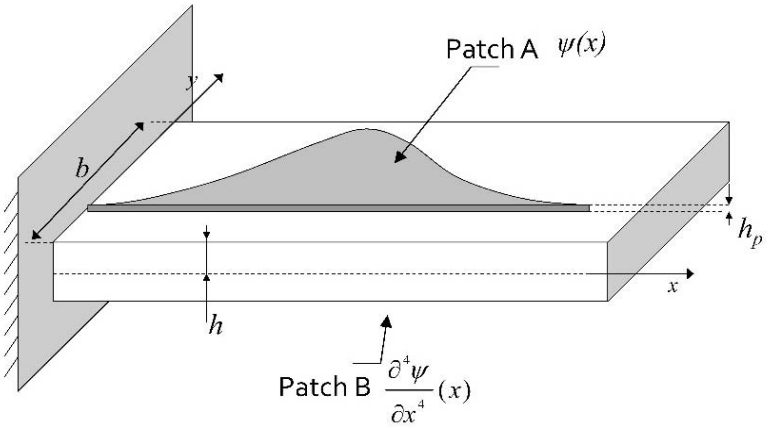

Fig. 1 Example of patches A and B glued on opposite sides of the beam

$$\Lambda(0) = +\mu\omega^2 \underbrace{\int_0^a \frac{\partial^2 w}{\partial x^2}(x)\Psi(x)dx}_{Mass\ patch} - E_b I \underbrace{\int_0^a \frac{\partial^2 w}{\partial x^2}(x)\frac{\partial^4 \Psi}{\partial x^4}(x)dx}_{Stiffness\ patch} \tag{10}$$

The coefficients $\mu\omega^2$ and E_bI can then be introduced through an amplification step in the acquisition process. Note that for the stiffness patch, the sign of the width can be negative. In technical terms, this patch is manufactured in various in dependent parts, the sign inversion can be achieved during the amplification step. Note also that the stiffness path is particularly sensitive in the low frequency domain (when the path length is small compared to the wavelength) whereas the mass patch becomes the most important in the high frequency domain due to the presence of the coefficient ω^2. This remark is illustrated in Fig. 2 issued from simulations presented in (Chesne and Pezerat 2011). It illustrates the manner in which the information is distributed with respect to wavelength, in the integration domain. The blue dottedline and the red continuous line represent respectively the relative contribution of the mass patch and the stiffness patch. As expected, when the patch lengths are small compared to the wavelength (less than half a wavelength in the integration domain), the useful signal is delivered entirely by the stiffness patch. Indeed, the stiffness patch is associated with the strain energy, which is the most significant form of energy in the low frequency domain (where the natural wavelength is high). When the wavelength is near the patch length, both patches participate, and the measured signals are important. This increase in amplitude of the measured signals, and the fact that the signals have opposite signs, tends to make the approach more sensitive to noise by amplifying it. Otherwise, when the patch lengths are greater than two wavelengths, the mass patch contribution becomes significant. These limits depend on the length of the patch. As an example, for a 10 cm long patch and for a steel beam (section:40*6 mm), the length of the sensor is equal to half a wavelength at 1400 Hz, one wavelength at 5500 Hz, and two wave lengths at 22500 Hz.

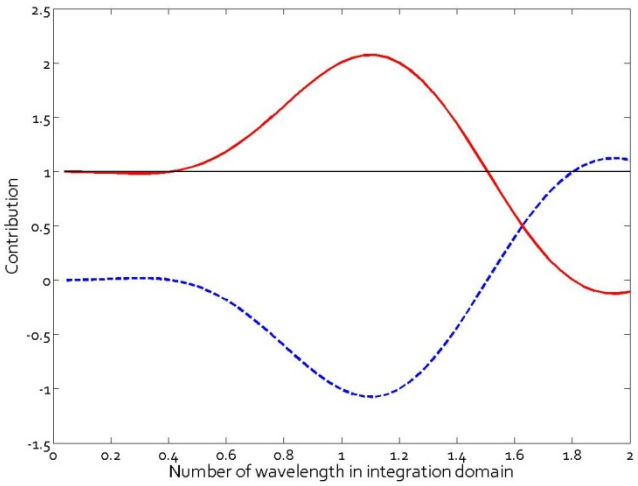

Fig. 2 Relative contributions of each patch to shear force identification (Mass patch: Blue dotted line, Stiffness patch: Continuous red line), from (Chesne and Pezerat 2011)

3. Experimental validations

3.1 Setup

A cantilever steel beam (length: 46 cm, width: 40 mm, thickness: 6 mm) is instrumented with piezoelectric bi-oriented PVDF films, whose widths are cut according to the functions $\psi(x)$ and $\frac{\partial^4 \psi}{\partial x^4}$. Sensors are shown on Fig. 3. For the sake of simplicity and also to limit the effects of undesired modes, it has been chosen to design sensors with central symmetries. Their characteristics are

- Young's modulus: $2.5GPa \pm 20\%$,
- Piezoelectric constants: $d31 = d32 = 6pC/N \pm 20\%$,
- Thickness: $40\mu m \pm 5\%$.

The sensors are *10 cm* long, they are bonded at the free end of the beam where a shaker is also fixed and excites the structure. The excitation signal is a random noise. A piezoelectric force sensor is also used to measure directly the force excitation. The fact that the excitation is located at the free boundary of the beam implies that the shear force at the boundary point is identical to the excitation force. So, the PVDF sensors are placed in order to identify this force and the results can be compared to the directly measured force.

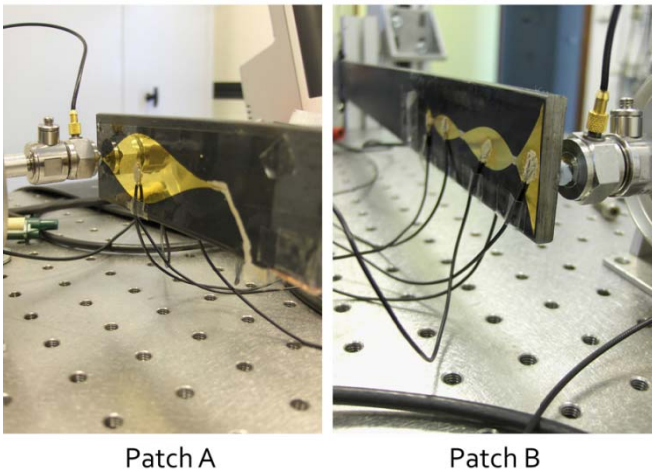

Fig. 3 Both sides of the instrumented beam. A: Mass patch, B: Stiffness patch

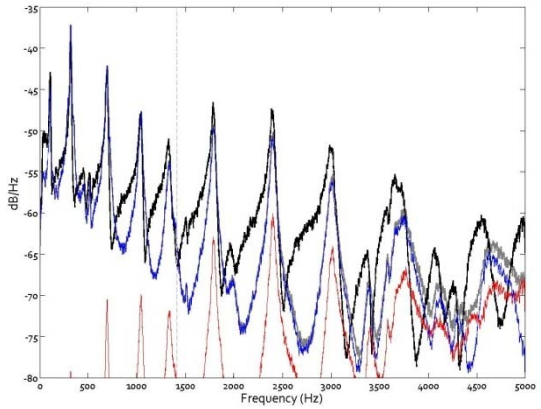

Fig. 4 Power spectral density [0-5000 Hz] of the measured force (black line), the complete reconstruction (grey line), Stiffness patch contribution (blue line) and mass patch reconstruction (red line). (ref: 1N)

3.2 Results

Fig. 4 shows spectra obtained for the large frequency range [0-5000 Hz]. The black curve corresponds to the directly measured force and constitutes a reference. The grey curve corresponds to the complete identification obtained from the combination of both signals as described by Eq. (10). The blue curve and the red curve correspond to the participation of the stiffness patch and the mass patch respectively. A vertical grey dotted line was also added to mark a frequency around *1400 Hz* for which the natural wavelength is equal to twice the length of the sensors (*2x10 cm*). This means that the integration domain contains a half wavelength. Even if a white noise was used,

spectra (and mainly the reference spectrum) show an important modal behaviour. This behavior is seen in the force excitation spectrum because there is a hard coupling between the shaker and the beam. Observed peaks correspond to the eigen modes of the coupled mechanical system, so, the measured reference force is more exactly the coupling force between the shaker and the beam.

Below 1400 Hz, the identification is particularly good on peaks, but significant differences appear for small values. These differences can be explained by many practical reasons: the uncertainties on the physical parameters of the PVDF films, the glue and the bonding process or the presence of a point force where the Saint Venant's principle is not locally respected. The participation of the mass sensor is theoretically negligible when the wavelength is greater than twice the length of the patch (see Fig. 2 or Chesne and Pezerat (2011)), that means it can be useless for low frequencies. The big interest of using only the stiffness patch is that it becomes to be possible to use the sensor without frequency decomposition, i.e., to use it in the time domain and in the real time. For frequencies higher than 1400 Hz, the identification starts to be less accurate (an error around 5dB) and clearly wrong after 4000 Hz. We assume the uncertainties described previously affect the reconstruction and are amplified on this frequency range as explained in section 2.3, but the main reason is the apparition of modes not modelled by the Euler-Bernoulli theory. The assumption of a pure bending behaviour used for the sensor design (Eq. (1)) is no more valid at these frequency ranges.

Figs. 5 and 6 show spectra and the phase differences obtained for a smaller frequency range *[0-1500Hz]*. Shear forces at the first five resonances (marked with small circles in Figs. 5 and 6) are well reconstructed and Table 1 gives the values of amplitudes and relative phases between the reference force sensor and the reconstructed force. Table 1 also gives the Number of Wavelengths in the Integration Domain (NoWID) for the given frequencies, quantifying the number of spatial periods inside the integration domain. Its expression is

$$NoWID = \frac{a}{\lambda} = \frac{ka}{2\pi} \tag{11}$$

where a is the sensor length, λ is the wavelength and k is the flexural wave number.

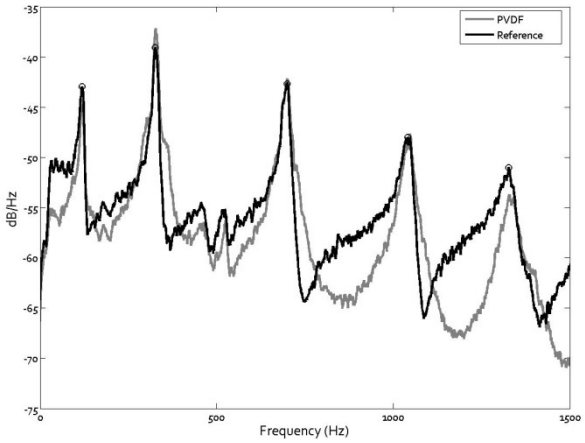

Fig. 5 Power spectral density [0-1500 Hz] of the measured force (black line) and the reconstructed force (grey line), resonances are marked with 'o'. (ref: 1N)

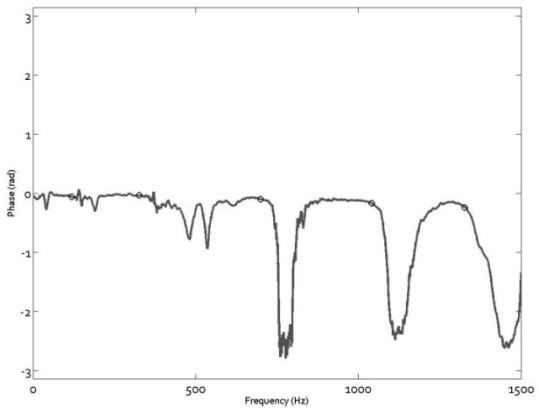

Fig. 6 Relative phase between the force sensor and the reconstructed force, resonances are marked with 'o'

Table 1 Number of Wavelengths in the Integration Domain (NoWID), Amplitude and phase comparison for the 5 first bending modes

Frequency (Hz)	118	327	705	1041	1329
NoWID	0.14	0.24	0.35	0.42	0.48
Amplitude (dB)	-1.6	+1.8	+0.5	+0.4	-2.6
Phase (rad)	-0.06	-0.03	-0.1	-0.17	-0.24

For the first four resonances, the differences of modulus are less than *2 dB* and the phase differences do not exceed *0.2 rad*. For the fifth resonance, increasing in differences appears to be more important. Note that the uncertainties on the characteristics of PVDF Film used for the sensor can have important effects. Even with these high uncertainties, the FISH seems to give a good accuracy on results.

As mentioned above, and shown in Fig. 2, in the low frequency domain, i.e., when the sensor length is smaller than half a wavelength, the stiffness patch can be used alone. A band limited random noise test *[0-500 Hz]* was also studied to see the identification in the time domain. Fig. 7 shows the signals obtained from the force sensor (black line) and the stiffness patch (thick dotted grey line) in real-time during *0.03s*. Both signals are similar, the most differences appear at some maxima.

To complete these observations, frequency range of the excitation has been extended to *[0-5000Hz]*. Fig. 8 shows the signals obtained from the force sensor (black line) and the stiffness patch (thick dotted grey line) in real-time during *0.03s*. The curves are close and the global low frequency behaviour is well identified. Only a few small details and peaks are not well reconstructed. This confirms the previous observations on the role of each patch.

These two last figures demonstrate that when the dynamic behaviour is globally dominated by the first flexural modes, the FISH sensor gives a result close to that of the reference sensor.

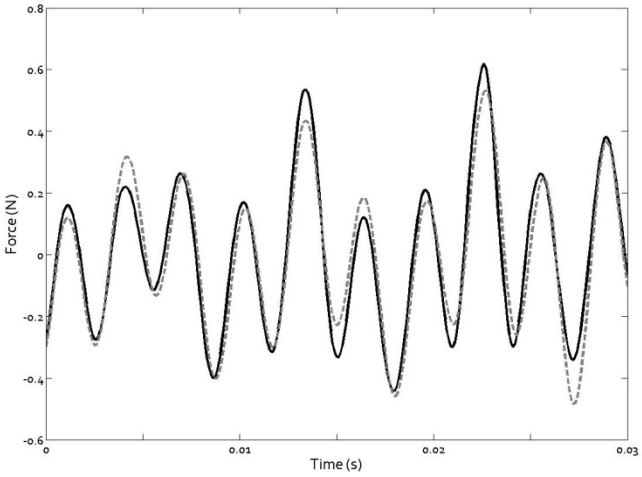

Fig. 7 Real time measurement, measured force (black line) and reconstructed force using only patch B (grey line). Limited frequency range excitation [0-500Hz]

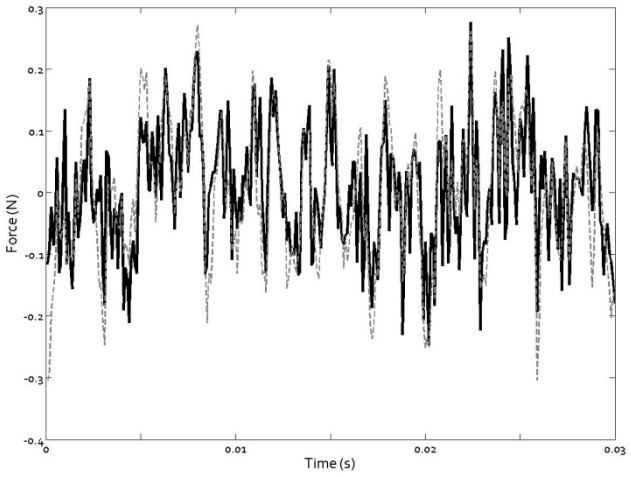

Fig. 8 Real time measurement, measured force (black line) and reconstructed force using only patch B (grey line). Large frequency range excitation [0-5000 Hz]

4. Conclusions

This paper has given a first experimental validation of the use of specific forms of PVDF patches for the assessment of spatial derivatives of the displacement field. The studied case is that of the shear force measurement, which constitutes the worst case since it is proportional to the third derivative of the displacement. This new kind of sensor presents the advantage to be flat, and

can also measure forces or derivatives at boundaries where these quantities are not readily accessible. In order to have a comparison, the shear force is assessed at a free boundary of a beam where an external force is applied by a shaker equipped with a standard piezoelectric force sensor. In order to develop a complete sensor available at several frequencies, the sensor is divided in two patches: the stiffness patch and the mass patch. The use of both allows one to obtained good results on a large frequency domain without exceeding differences of *2dB* in modulus and *0.2 rad* in phase with respect to the reference. In the low frequency domain, when the natural wavelength of the beam is larger than twice the sensor length, the stiffness patch can be used alone, this gives the interest to have a frequency-independent gain and allows one to use it in real time.

Extensions to more complex structure or other motions (like torsion) require finding adequate test functions and positions of the patch. The actual and main scientific difficulty is when the equation of motion contains 2D spatial derivatives and/or cross derivatives (as for Kirchhoff plates) where two dielectric displacement vectors have to be taken into account and where the concrete implementation of the 2D test function must be imagined.

References

Ablitzer, F., Pézerat, C. and Génevaux, J.M. (2012), "Identification of the damping ratio of multi-layered composite panels from the verification of their local equation of motion", *Proceedings of the Vibrations, Shock and Noise*, Clamart, France.

Chesné, S., Pézerat, C. and Guyader, J.L. (2006), "Identification of boundary forces in beams from measured displacements", *J. Vib. Acoust*., **128**(6), 757-771.

Chesné, S., Pézerat, C. and Guyader, J.L. (2008), "Identification of plate boundary forces from measured displacements", *J. Vib. Acoust.*, **130**(4), 041006-1.

Chesné, S. and Pézerat, C. (2011), "Distributed piezoelectric sensors for boundary force measurements in Euler Bernoulli beams." *Smart Mater. Struct*.**20**, 075009, 1-9.

Chochol, C., Chesné, S. and Remond, D. (2013), "An original differentiation tool for identification on continuous structures", *J. Sound Vib.*, **332**(13), 3338-3350.

Clark, R.L. and Burke, S.E. (1996), "Practical limitations in achieving shaped modal sensors with induced strain materials", *J. Vib. Acoust*., **118**(4), 668-675.

François, A., De Man, P. and Preumont, A. (2001), "Piezoelectric array sensing of volume displacement: a hardware demonstration", *J. Sound Vib*., **244**(3), 395-405.

Friswell, M.I. (2001), "On the design of modal actuators and sensor", *J. Sound Vib.*, **241**(3), 361-372.

Gavric, L. and Pavic, G. (1993), "Finite element method for computation of structural intensity by normal mode approach", *J. Sound Vib.*, **164**(1), 29-43.

Gawronski, W. (2000), "Modal actuators and sensors", *J. Sound Vib.,* **229**(4), 1013-1022.

Grédiac M. (1989), "Principe des travauxvirtuels et identification [principle of virtual work and identification", *Comptes Rendus de l'Académie des Sciences*, **309**(1-5), In French with abridged English version.

Gu, Y., Clark, R.L., Fuller, C.R. and Zander, A.C. (1994), "Experiments on active control of plate vibration using piezoelectric actuators and polyvinylidene fluoride (pvdf) modal sensor", *J. Vib. Acoust*., **116**(3), 303-308.

Guyader, J.L. (2002), *Vibration in Continuous Media*, Wiley-Blackwell, ISTE, Chippenham, England.

Hubbard, J.E. (2010), *Spatial Filtering for the Control of Smart Structures*, Springer-Verlag Berlin Heidelberg..

Leclère, Q. and Pézerat, C. (2012), "Vibration source identification using corrected finite difference schemes", *J. Sound Vib.*, **331**(6), 1366-1377.

Lee, C.K. and Moon, F.C. (1990), "Modal Sensors/actuators", *J. Appl. Mech. -T ASME*, **57**, 434-441.

Noiseux, D.U. (1970), “Measurement of power flow in uniform beams and plates”, *J. Acoust. Soc. Am.*, **47**(18), 238-247.
Pavic, G. (1976), “Measurement of structure borne wave intensity, Part I: Formulation of the methods”, *J. Sound Vib.*, **49**(2), 221-230.
Pézerat, C. and Guyader, J.L. (1995), “Two inverse methods for localization of external source exciting a beam”, *Acta Acustica*, **1**(3), 1-10.
Pézerat, C. and Guyader, J.L. (2000), “Force analysis technique: Reconstruction of force distribution on plates”, *Acta Acustica*, **86**(2), 322-332.
Pierron, F. and Grédiac, M. (2012), *The Virtual Fields Method*, Springer, New-York.
Preumont, A., François, A., De Man, P. and Piefort, V. (2003), “Spatial filters in structural control”, *J. Sound Vib.*, **265**(1), 61-79.
Xu, H., Cheng, L., Su, Z. and Guyader, J.L. (2011), “Identification of structuraldamage based on locally perturbed dynamic equilibrium with an application tobeam component”, *J. Sound Vib.*, **330**, 5963-5981.
Zhang, Y. and Adin Mann, J., III, (1999), “Measuring the structural intensity and force distribution in plates”, *J. Acoust. Soc. Am.*, **99**(1), 345-361.

FC